56-20
N96-70527
J.27
P-12

# ARCJET PLUME DIAGNOSTICS

W. M. Ruyten*
*University of Tennessee-Calspan*
*Center for Space Transportation and Applied Research*
*Tullahoma, Tennessee 37388-8897*

and

D. Keefer**
*Center for Laser Applications*
*University of Tennessee Space Institute*
*Tullahoma, Tennessee 37388-8897*

**Abstract**

*We report the results of spectroscopic measurements on the exhaust plume from a 1 kW NASA Lewis arcjet, operated on simulated ammonia. The strongest emission features consist of the Balmer lines of atomic hydrogen and a number of vibration-rotation bands of the NH radical. From the spectral data, we calculate a heavy particle temperature of about 3000 K at the exit plane, and an electron temperature of 0.30 eV. Measurements of the spatial distribution of these emission features are presented also. We discuss the importance of the measurements to planned laser induced fluorescence experiments.*

## 1. Introduction

With the upcoming deployment of hydrazine arcjets on the 1993 launch of Telstar 4, arcjets have reached the point of commercial viability. Still, a strong interest remains in improving their performance. To a significant extent, this effort is hampered by the limited understanding of the basic physical processes in the device. This accounts for the continuing interest in experimental diagnostics and numerical modeling.

Different techniques have been used to characterize arcjet plumes. These include Langmuir probes [1-2], emission spectroscopy [3-8], absorption [9-10], and laser induced fluorescence (LIF) [8,11-15]. Emission spectroscopy has also been used to monitor the arc region itself [16]. At the same time, there have been several modeling efforts [17-19]. The combined experimental and numerical work is providing greater insight into the mechanisms of arc physics, the generation of thrust, and the factors determining electrical efficiency of the device.

We have previously demonstrated the LIF technique on a locally-built arcjet, operated on argon [13-15]. The main goal of the present effort is to perform similar measurements on the plume from a 1 kW benchmark thruster from NASA Lewis Research Center [20], operated on simulated ammonia (a mixture of three parts hydrogen to one part nitrogen by volume). The excitation line that will be used for these LIF studies is the Balmer-alpha line of atomic hydrogen at 6563 Å.

Because of scheduling conflicts, we have not yet been able to perform the LIF studies themselves. However, spectroscopic investigations of the plume were performed in preparation for the LIF work. Although these measurements were intended primarily as a stepping stone toward the more complicated LIF experiments, they are interesting in their own right. In particular, these measurements were not restricted to the hydrogen Balmer-alpha line. Strong emissions were also observed from other members of the hydrogen Balmer series, and several strong vibrational-rotational bands of the NH radical were detected.

Here we demonstrate how these emissions can be used to map the spatial distributions of H and NH in the plume,

This work was supported jointly by Rocket Research Company of Redmond, WA; the Air Force Office of Scientific Research; and by the Center for Space Transportation and Applied Research.

* Principal Investigator; Calspan, Senior Engineer
** UTSI/CLA, B. H. Goethert Professor of ES&M

and to determine plume temperatures. We report the results of three different temperature determinations. The first is analysis of the Doppler width of the hydrogen Balmer-alpha line. This yielded a temperature of 3150 ± 80 K at the nozzle exit plane. The second is determination of the electron temperature from the intensity ratios of the hydrogen Balmer-beta through Balmer-epsilon lines. This resulted in a temperature of 0.300 ± 0.003 eV, or 3470 ± 35 K. Finally, the rotational temperature of the NH $c^1\Pi \rightarrow b^1\Sigma^+$ (0-0) band was determined to be 2680 ± 60 K.

The close agreement between these three independent temperature determinations is striking. However, this situation may be peculiar to the high chamber background pressure in this work (500 Pa, or 4 Torr). At the time of the LIF measurements, additional pumping will be available, resulting in an estimated chamber pressure of about 50 Pa. It should be worthwhile to repeat the spectroscopic measurements at that time.

The outline of this paper is as follows: Section 2 describes the experimental setup and procedures for the spectroscopic work. In Section 3 we describe the measurements on the hydrogen Balmer lines, including line shape analysis of the Balmer-alpha line and the determination of electron temperature from the Balmer-beta through Balmer-epsilon lines. In Section 4 we present measurements of the rotational bands of the NH radical, and the determination of the rotational temperature of the $c^1\Pi \rightarrow b^1\Sigma^+$ (0-0) band. In Section 5, we discuss measurements of the spatial distributions of excited H and NH emissions. In Section 6 we conclude with a summary and a discussion of the relevance of the data to future arcjet plume studies.

## 2. Experimental

All experimental work was performed in the large vacuum facility of the Center for Laser Applications at the University of Tennessee Space Institute. The vacuum tank consists of a cylindrical chamber, 6.0 m long by 2.7 m wide, with a bell-shaped section on one end. This is where the arcjet was mounted, namely on a computer-controlled xyz stage (see Fig. 1). For these experiments, only a single Stokes pump equipped with blower was available, with a pumping speed of 110 l/s. Typical vacuum levels during thruster operation were 400 to 670 Pa (3 to 5 Torr), at flow rates of 5 to 7 sl/min.

Figure 2 shows the arcjet, which is on loan from NASA Lewis Research Center. A description of the arcjet may be found, for example, in Ref. [20]. Typical power dissipation was 10 Amps at 80 Volts, for a flow rate of 7 sl/min. The 3:1 hydrogen-nitrogen mixture was premixed. The mixture was chosen to avoid dealing with the corrosive properties of ammonia itself. A comparison with operation on actual ammonia may be undertaken at a future date. Based on experiments performed at Aerospace Corporation [8] we expect only minor differences between operation on actual versus simulated ammonia.

The emission measurements were performed with a 1.25 meter SPEX spectrometer with an 1800 gr/mm grating. Typical slit widths were 10 μm and 25 μm, with corresponding resolutions of 0.038 Å and 0.095 Å, measured as full-width-half-maximum (fwhm) values on an assumed gaussian instrument line profile. Emissions from the plume were collected through a large optical access port in the chamber, and focused onto the spectrometer entrance slit with a wide-aperture (f/6) Cassegrain telescope.

A red-sensitized photo multiplier tube (PMT) was used as the detector. The quantum efficiency of this tube falls off sharply above 8600 Å. Light below 3300 Å is not transmitted by the optical access port of the chamber. Figure 3 shows the combined detection efficiency of the optical setup. This calibration was performed with a standard filament source, which was placed at the position of the arcjet plume for this purpose.

The dominant spectral features in the emission spectra of the arcjet plume were those of atomic hydrogen (Section 3) and the NH radical (Section 4). Also, weak emissions from the molecular nitrogen ion ($N_2^+$) were present, with a bandhead at 3914 Å, stretching to the blue. No emissions from atomic nitrogen could be detected.

A drawback of the use of the Cassegrain telescope turned out to be its use of a diffractive element. This resulted in a net shift of the effective observation point in the plume as a function of observation wavelength. This effect is particularly noticeable in the spatial plume measurements of Section 5. However, it may also be that because of this effect the calibration curve from Fig. 3 is slightly in error, as is discussed at the end of Section 3.

## 3. Analysis of hydrogen Balmer emissions

One of the strongest emission features in the plume was the series of lines corresponding to the Balmer series of atomic hydrogen. As is illustrated in Fig. 4, this is the series of lines which terminate on the level with principal quantum number equal to two (n=2). The most prominent of these is the Balmer-alpha line at 6563 Å, which corresponds to the n=3 to n=2 transition. Also observed were the beta (4→2), gamma (5→2), delta (6→2), epsilon (7→2), and zeta (8→2) members of this series.

Figure 5 shows a scan of the Balmer-alpha line. This measurement was performed about 2 mm downstream from the exit nozzle, with slit settings of 25 μm. The asymmetry of the line shape is a result of the fine structure of the line. Due to this fine structure, the Balmer-alpha line actually consists of five non-overlapping components, with relative positions of -0.144, -0.036, 0.0, 0.220, and 0.328 $cm^{-1}$, and corresponding intensity ratios of 0.05 : 0.28 : 2.50 : 0.31 : 1.96 [12, 21, p.223].

We were able to fit the lineshape from Fig. 5 (solid line) almost perfectly by a multi-component gaussian curve fit (dotted line), in which each component (dashed lines in Fig. 5) represents one of the five non-overlapping fine structure transitions. The relative positions and relative amplitudes are as specified above, and the width of each of the components is the same. The fitted value of this width at fwhm is 0.2807 ± 0.0002 Å. Correcting for the spectrometer width of 0.095 Å, we find that the Doppler width of the transition, $\Delta_D$, is 0.2641 Å fwhm. Substituting this value into the expression for Doppler broadening:

$$8\ k\ T\ \ln 2 = m\ c^2\ (\Delta_D / \lambda)^2, \qquad (1)$$

where k is Boltzmann's constant, λ is the transition wavelength, and m is the mass of atomic hydrogen, we find a value of the Doppler temperature, T, of 3150 K. The main uncertainty in this value is due the correction for the instrument width. Estimating this uncertainty to be 10 percent, it follows that the uncertainty in the Doppler temperature is 80 K.

We have also performed scans of the Balmer-beta through Balmer-zeta lines. No fine structure analysis was performed for these lines. However, Table I lists the calculated areas and widths of these lines, as well as several other quantities. Also, the corresponding quantities for the Balmer-alpha line are shown. From these data, it is possible to estimate the electron temperature in the plume [3].

This is illustrated in Fig. 6, in which the log of the ratio $S_i^*/S_\infty$ is plotted versus the upper state energy $E_i$ of the transition, where $S_\infty$ is a measure (in arbitrary units) of the line intensity in the limit of infinite temperature [21, p.129], and $S_i^* = S_i/\eta_i$ is the measured line intensity $S_i$ corrected for the detection efficiency $\eta_i$ from Fig. 3 at the specified wavelength. From the expression

$$S_i^* \propto S_\infty \exp(-E_i / kT_e), \qquad (2)$$

it follows that the data in Fig. 6 should fall on a straight line whose slope is inversely proportional to the electron temperature $T_e$.

It is clear from Fig. 6 that the data from the Balmer-beta through Balmer-epsilon lines fall on a straight line indeed. The slope of this line yields an electron temperature of 3470 ± 35 K, or 0.300 ± 0.003 eV. The data point for the Balmer-zeta line was not included in the linear fit because we believe that this line overlaps with a rotational line from the molecular nitrogen ion, which was present in small amounts. Neither was the data point for the Balmer-alpha line included in the fit, due to its evidently anomalous behavior relative to the other lines from the Balmer series.

One possible explanation for the anomalous behavior of the Balmer-alpha line is that the sensitivity calibration from Fig. 3 is in error as a result of the diffractive effects of the Cassegrain telescope. As discussed at the end of Section 2, such diffractive effects might have been responsible for focusing different portions of the standard-lamp-filament onto the entrance slit of the spectrometer. This would affect the Balmer-alpha point in Fig. 6 in particular, because its sensitivity factor ($\eta_i$ = 2.841) differs so much from the factors for the Balmer-beta through Balmer-epsilon lines (each equal to 80 within a few percent - see Table I).

The measured value of 0.30 eV for the electron temperature is in good agreement with electron temperature measurements in arcjet plumes obtained with Langmuir probes [1-2]. Also, it is in excellent agreement with the value of 0.33 eV obtained in Ref. [3], obtained using the same method as that employed here. Interestingly, the Balmer-alpha point was excluded in Ref. [3] as well, where it fell significantly *below* the straight line fitted through the other data points.

We conclude this section by reiterating that the hydrogen Balmer-alpha line was found to be the most prominent emission feature in the plume spectrum. Thus we are confident that the population of the n=2 level in Fig. 4 will be sufficient to excite the Balmer-alpha transitions in an LIF experiment as well.

### 4. Analysis of NH molecular bands

In addition to the strong series of lines of the hydrogen Balmer series, strong emissions from the NH radical were found. The most prominent, and perhaps most characteristic, of these are those of the $A^3\Pi \rightarrow X^3\Sigma^-$ band. Figure 7 shows a partial scan of this band system. The Q-branches of the 0-0 and 1-1 vibrational transitions are identified in the left part of Fig. 7. The remaining part of the scan reveals the interwoven P-branch transitions of the 0-0 and 1-1 systems.

The NH A→X band has been studied previously by Crofton et al., namely in the plume from an ammonia arcjet, similar to the one used in our work [8]. Both emission and excitation measurements were performed. A surprising finding of Ref. [8] was that the rotational temperatures calculated from the emission spectra, around 4500 K, were significantly higher than those of the excitation spectra, which were only about 2000 K. Also, the vibrational temperature, estimated from the ratio of 1-1 to 0-0 emissions, was significantly lower, namely 2500 K. However, it is also stated in Ref. [8] that these temperature determinations have a considerable uncertainty, due to an apparent violation of Boltzmann equilibrium among the rotational levels.

Similar analyses could be performed on the data from Fig. 7, yielding rotational temperatures for both the 0-0 and 1-1 bands. Also it should be possible to estimate a vibrational temperature from the 0-0 to 1-1 emission ratios. We have the resources to perform this type of analysis, but have not done so yet. However, from a mere comparison of the spectrum from Fig. 7 with the spectra shown in Ref. [8], it appears that the vibrational temperature must be higher than 2500 K (the 1-1 transitions have larger relative amplitudes in Fig. 7 than in the corresponding figures from Ref. [8]). Similarly, the significant representation of transitions with large rotational quantum numbers (the lines above about 343 nm in Fig. 7) appears to indicate that the rotational temperature is probably not much lower than the value of 4500 K found in Ref. [8].

Other band systems of NH were observed in our work as well. These include the (0-1) band of the $A^3\Pi \rightarrow X^3\Sigma^-$ system between 370 and 381 nm; the (0-1) band of the $c^1\Pi \rightarrow a^1\Delta$ system between 363 and 367 nm; and the (0-0) band of the $c^1\Pi \rightarrow b^1\Sigma^+$ system between 450 and 474 nm. A comprehensive discussion of these various band systems may be found in Ref. [22], which shows spectra obtained in an ammonia-argon arcjet plume.

We did perform an analysis of the $c^1\Pi \rightarrow b^1\Sigma^+$ band. A scan of the main part of this band is shown in Fig. 8. Because the band involves singlet transitions, the line structure is much more open than that of the triplet $A^3\Pi \rightarrow X^3\Sigma^-$ band. This simplifies the analysis considerably. In particular, it is straightforward to measure the intensities of individual rotational transitions and to obtain the rotational temperature, $T_R$, of the plume. This is accomplished in a similar fashion as for the above analysis of the hydrogen Balmer series. In particular, the expression which corresponds directly to Eq.(2) is given by

$$S^*(J') \propto S_{J'J''} \exp ( -E(J') / kT_R ), \qquad (3)$$

where $S^*(J')$ is the line intensity of the line with rotational quantum number J', corrected for the optical detection efficiency; $S_{J'J''}$ is the Hönl-London line strength factor; and E(J') is the energy of the upper rotational level. Expressions for the line strength factors were taken from Ref. [23]. They are given by $S_{J'J''} = \frac{1}{2}J'$ for the P-branch; $S_{J'J''} = J'+\frac{1}{2}$ for the Q-branch; and $S_{J'J''} = \frac{1}{2}(J'+1)$ for the R-branch transitions.

The resulting Boltzmann plot for the $c^1\Pi \rightarrow b^1\Sigma^+$ band is shown in Fig. 9. The line intensities were measured directly off the stripchart output from the survey scan of the spectrum. A total of 41 isolated transitions were identified, namely 10 from the P-branch, 17 from the Q-branch, and 14 from the R-branch. A linear fit to the data yields a rotational temperature of $T_R = 2680 \pm 60$ K, and is seen to approximate all data reasonably well. Based on this observation, we conclude that the assumption of Boltzmann equilibrium is well justified for these data (the opposite conclusion was drawn in Ref. [8]).

### 5. Spatial distribution of emission intensities

Several experiments were performed to characterize the spatial distribution of emission intensities in the plume. For this purpose, the spectrometer was tuned to a particular emission line, and a scan was performed by moving the arcjet thruster either parallel or perpendicular to the plume axis. The entrance and exit slits of the spectrometer were opened to 200 μm and 400 μm, respectively, to include most of the area under the emission lineshape.

Figure 10 shows the variation in emission signal for the alpha, beta, and gamma lines of the hydrogen Balmer series. Also shown is the signal at 336 nm, given by the (0-0) Q-branch of the A→X band of NH. All data were scaled to unit amplitude. It appears that the spatial behavior of all components is different. In part, this is due to the refractive distortion of the Cassegrain telescope, which resulted in wavelength-dependent relative shifts of the emission profiles. Thus, unfortunately, the value of the data from Fig. 10 is limited.

One unambiguous conclusion from Fig. 10 is that NH emission persists long after the hydrogen Balmer emissions have subsided. Also, the width of the Balmer-alpha profile is less than that of the Balmer-beta profile. In turn, its width is less than that of the Balmer-gamma profile. In principle, it should be possible to calculate from this the axial variation of the electron temperature, using Eq.(2). However, this will not be possible until the wavelength-dependent distortion of the Cassegrain telescope is remedied or accounted for.

Similarly, Figure 10 shows the radial variations of the Balmer-alpha emission and the NH Q-branch emission, several millimeters downstream from the exit nozzle. In these measurements, the optical distortion is even more evident: Clearly, there is no reason why the two emissions should be centered differently around the plume axis. Figure 10 also points out another difficulty in obtaining good spatial measurements with the Cassegrain system: the asymmetry of the radial Balmer-alpha profile. In a modest effort it was established that the profile is quite sensitive to the alignment of the optical system.

We conclude that it is straightforward to get a rough idea of the spatial distribution of emitting plume species from the axial and radial scans. However, a very careful optical alignment will be required for quantitative measurements. Moreover, it will be desirable to replace the present Cassegrain system with one without diffractive optics. Because it is likely that the spatial distributions of emitting plume species will be affected to a significant extent by the lower background pressure that we anticipate for future experiments, we did not perform any further spatial distribution measurements.

## 6. Discussion and summary

We have performed spectroscopic measurements on the plume from a 1 kW arcjet, operated on simulated ammonia. The resolution of these measurements was better than 0.1 Å. Thus, three independent plume temperature determinations could be performed. These were based on the Doppler width of the hydrogen Balmer-alpha line; the intensity ratios of the hydrogen Balmer-beta through Balmer-epsilon lines; and the rotational line intensities of the (0-0) branch of the $c^1\Pi \rightarrow b^1\Sigma^+$ band of the NH radical. The respective temperatures at the exit plane, 3150 ± 80 K, 3470 ± 35 K, and 2680 ± 60 K are in close agreement.

It must be kept in mind that these values are averaged quantities along the line-of-sight. Thus it is difficult to extract local values of temperatures and concentrations from them, although such could be accomplished by Abel inversion of radial emission profiles [3]. However, the method of choice for obtaining such point data is laser induced fluorescence (LIF). We plan to perform such LIF experiments in the near future, using the hydrogen Balmer-alpha line.

Because of its prominence as an emission feature, we are confident that the hydrogen Balmer-alpha line can be used as a valuable diagnostic line in LIF experiments as well. However, the emission measurements also point out a concern in this regard, namely the apparently anomalous behavior of the emission intensity of the hydrogen Balmer-alpha line relative to the higher members of the Balmer series.

Such anomalous behavior has been reported elsewhere as well [3]. It appears that the population of the n=3 state (the upper level of the Balmer-alpha transition in emission) is *not* in thermal equilibrium with the other members of the Balmer series. However, its Doppler temperature seems to agree both with the distribution of higher-level quantum states of the H atom as well as with the distribution of rotational levels of the $c^1\Pi$ v=0 branch of the NH radical.

Because excitation of the Balmer-alpha line in an LIF scheme involves an even lower level (the n=2 level), the possibility for anomalous behavior is even greater. Moreoever, the observed non-equilibrium effects in this work may have been mitigated by the rather high background pressure in the experiments. An upgrade of the vacuum facility is almost complete. Thus future experiments will be carried out at lower background pressures. For these, it will be even more important to compare the results from excitation measurements obtained with LIF to results obtained with emission spectroscopy.

Only one of the molecular bands of the NH radical was analyzed in this work, namely the $c^1\Pi \rightarrow b^1\Sigma^+$ (0-0) band. Its singlet structure allows for a simpler analysis than the triplet $A^3\Pi \rightarrow X^3\Sigma^-$ system, studied in Refs. [4] and [8]. In particular, it was easy to measure the intensities of individual rotational lines. Thus it was possible to obtain the rotational temperature from a Boltzmann plot which included all three branches (P, Q, and R) of the band system. The resulting temperature agrees well with the two temperatures obtained from the hydrogen Balmer emissions, and is roughly equal to that obtained from the emission measurements from Ref. [8].

An interesting feature of the NH emissions is that they persist at least 10 mm further downstream from the exit nozzle than the Balmer emissions from atomic hydrogen. This information may be useful to validate models of the plume chemistry. Also, weak emissions from the molecular nitrogen ion were detected. No emission from atomic nitrogen was found. Thus it seems very unlikely that excitation of atomic nitrogen using LIF could be used as a valuable diagnostic.

Finally, our experiments indicate that some modifications to the optical setup would be required to perform precise measurements of the spatial distributions of emission intensities. In particular, the wavelength-dependent distortion of the Cassegrain telescope would have to be eliminated or accounted for. However, the

measurements also indicate that, having made such a modification, it should be possible to measure the dependence of the electron temperature and Doppler temperature of the Balmer-alpha line as a function of downstream position from the exit nozzle.

### Acknowledgments

This work was supported by grants from Rocket Research Company of Redmond, Washington; the Air Force Office of Scientific Research under grant AFOSR-91-0200; and by the Center for Space Transportation and Applied Research under NASA grant NAGW-1195. We gratefully acknowledge the loan of the arcjet system from NASA Lewis Research Center. Finally, we thank N. Wright for his expert technical assistance.

### References

[1] Sankovic, J. M., "Investigation of the arcjet near field using electrostatic probes," NASA TM 103638, Washington, D.C., 1990.

[2] Carney, L. C., and Keith, T. G., "Langmuir probe measurements of an arcjet exhaust," *J. Propulsion and Power*, Vol. 5, No. 3, pp. 287-294, May-June 1989.

[3] Hoskins, W. A., Kull, A. E., and Butler, G. W., "Measurement of population and temperature profiles in an arcjet plume," AIAA paper 92-3240, Nashville, TN, July 1992.

[4] Janson, S. W., Welle, R. P., Schulthess, D. R., and Cohen, R. B., "Arcjet plume characterization part II: optical diagnostics results," AIAA paper 90-2643, Orlando, FL, July 1990.

[5] Manzella, D. H., Curran, F. M., Myers, R. M., and Zube, D. M., "Preliminary plume characteristics of an arcjet thruster," AIAA paper 90-2645, Orlando, FL, 1990.

[6] Tosti, E., Deininger, W. D., Mazzacurati, V., and Ruocco, G. C., "Arcjet plume analysis using emissions spectroscopy," paper 91-092, 22nd IEPC, Viareggio, Italy, October 1991.

[7] Cernogora G., et al., "Rotational temperature measurements of $N_2^+$ in an arcjet at low pressure," AIAA 92-2967, Nashville, TN, July 1992.

[8] Crofton, M. W., Welle, R. P., Janson, S. W., and Cohen, R. B., "Temperature, velocity, and density studies in the 1 kW ammonia arcjet plume by LIF," AIAA paper 92-3241, Nashville, TN, July 1992.

[9] Pollard, J. E., "Arcjet diagnostics by XUV absorption spectroscopy," AIAA paper 92-2966, Nashville, TN, July 1992.

[10] Manzella, D. H., and Cappelli, M. A., "Vacuum ultraviolet absorption in a hydrogen arcjet," AIAA paper 92-3564, Nashville, TN, July 1992.

[11] Erwin, D. A., Pham-Van-Diep, G. C., and Deininger, W. D., "Laser induced fluorescence measurements of flow velocities in high-power arcjet thruster plumes," *AIAA Journal*, Vol. 29, No. 8., 1991, pp. 1298-1303.

[12] Liebeskind, J. G., Hanson, R. K., and Cappelli, M. A., "Flow diagnostics of an arcjet using laser induced fluorescence," AIAA paper 92-3243, Nashville, TN, July 1992.

[13] Ruyten, W. M., and Keefer, D., "Characterization of electric thruster plumes using laser induced fluorescence measurements," AIAA paper 92-2965, Nashville, TN, July 1992.

[14] Ruyten, W. M., and Keefer, D., "Laser fluorescence velocimetry of an arcjet exhaust plume," paper 91-093, 22nd IEPC, Viareggio, Italy, October 1991.

[15] Ruyten, W. M., Friedly, V. J., and Keefer, D., "Electric propulsion: experimental research," Proceedings of the 3rd Annual Technical Symposium, Center for Space Transportation and Applied Research, Tullahoma, Tennessee, January 14-15, 1992, pp. 83-90.

[16] Zube, D. M., and Myers, R. M., "Techniques for spectroscopic measurements in an arcjet nozzle," *J. Propulsion and Power*, Vol. 8, No. 1, pp. 254-256, Jan.-Feb. 1992.

[17] Moeller, T., Rhodes, R., Keefer, D., Sedghi-Nasab, A., and Ruyten, W., "Comparison of experimental and numerical results for an argon arcjet," AIAA paper 92-3105.

[18] Rhodes, R. P., and Keefer, D., "Modeling of a hydrogen arcjet thruster," AIAA paper 91-1994, Sacramento, CA, June 1991.

[19] Tanaka, K., Tschiya, K., Kaita, K., and Nishida, M., "Computational simulation of arcjet thruster flow fields," paper A90-25826, 3rd International Symposium on Computational Fluid Dynamics, Nagoya, Japan, August 1989.

[20] Curran, F. M., and Sarmiento, C. J., "Low power arcjet performance characterization," AIAA paper 90-2578, Orlando, FL, July 1990.

[21] Kuhn, H. G., "Atomic Spectra," 2nd Ed., Academic Press, New York, 1969.

[22] Lents, J. M., "An evaluation of molecular constants and transition probabilities for the NH free radical," *J. Quant. Spectrosc. Radiat. Transfer*, Vol. 13, 1973, pp. 297-310.

[23] Kovacs, I., "Rotational structure in the spectra of diatomic molecules," American Elsevier, New York, 1969, p. 123.

**Table I:** Data obtained from scans of the hydrogen Balmer-alpha through Balmer-zeta lines. Listed from left to right are: (1) line designation and wavelength; (2) line width, $\Delta$, at fwhm; (3) integrated signal, $S_i$, under line profile; (4) intensity calibration factor, $\eta_i$, from Fig. 3; (5) corrected line intensity, $S_i^* = S_i/\eta_i$; (6) line intensity, $S_\infty$, in limit $T\rightarrow\infty$; (7) log ratio, $\ln(S_i^*/S_\infty)$, from Eq.(2); and (8) upper state energy, $E_i$. Numbers in parentheses indicate estimated standard deviations in the last digits.

| (1) Line | (2) $\Delta$ (Å) | (3) $S_i$ (mVÅ) | (4) $\eta_i$ | (5) $S_i^*$ (mVÅ) | (6) $S_\infty$ | (7) $\ln(S_i^*/S_\infty)$ | (8) $E_i$ (eV) |
|---|---|---|---|---|---|---|---|
| Hα: 6563Å | 0.3320(3) | 26601(35) | 2.841 | 9363(12) | 11.8 | 6.676(2) | 12.089 |
| Hβ: 4861Å | 0.2451(8) | 3656(17) | 82.75 | 44.2(2) | 5.38 | 2.106(5) | 12.750 |
| Hγ: 4341Å | 0.2343(37) | 682.1(1.4) | 80.08 | 8.52(2) | 2.87 | 1.088(2) | 13.056 |
| Hδ: 4102Å | 0.241(11) | 205(12) | 79.16 | 2.59(15) | 1.50 | 0.546(56) | 13.222 |
| Hε: 3970Å | 0.281(32) | 99(14) | 78.51 | 1.25(18) | 1.04 | 0.184(13) | 13.322 |
| Hζ: 3889Å† | 0.238(38) | 63(13) | 53.94 | 1.16(24) | 0.73 | 0.47(18) | 13.388 |

† Line thought to be coincident with rotational line from $N_2^+$ spectrum.

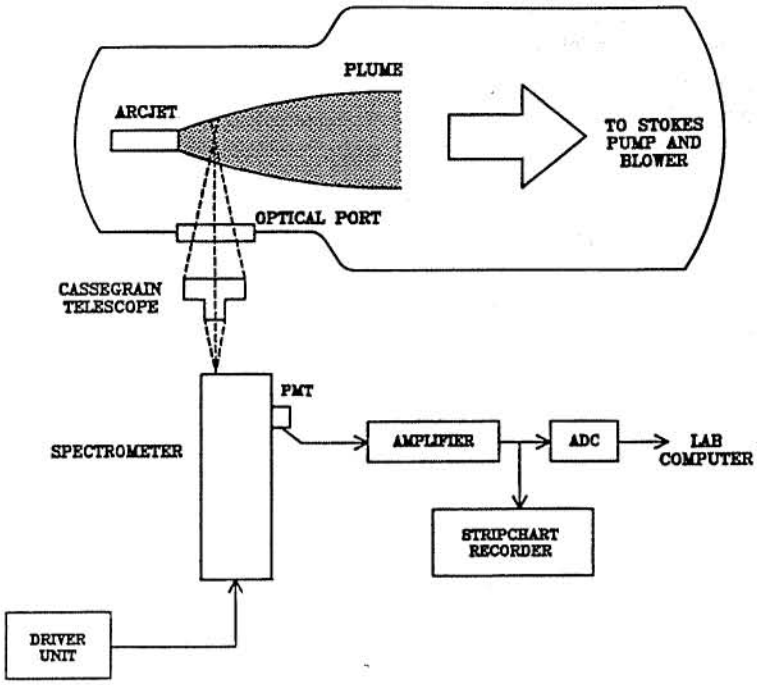


**Figure 1:** Schematic of the optical setup.

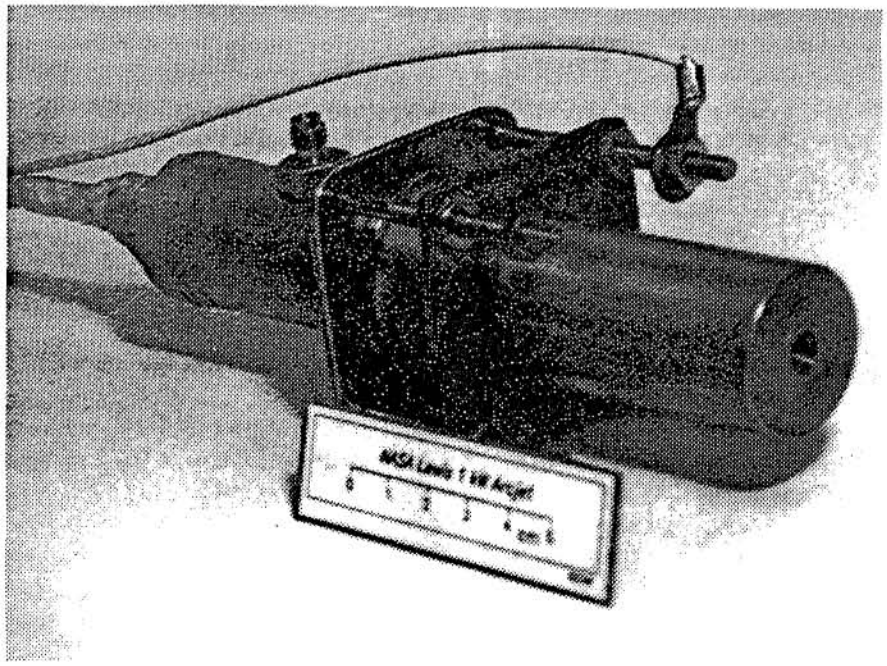

**Figure 2:** Photograph of the NASA Lewis arcjet. Length of displayed scale is 5 cm.

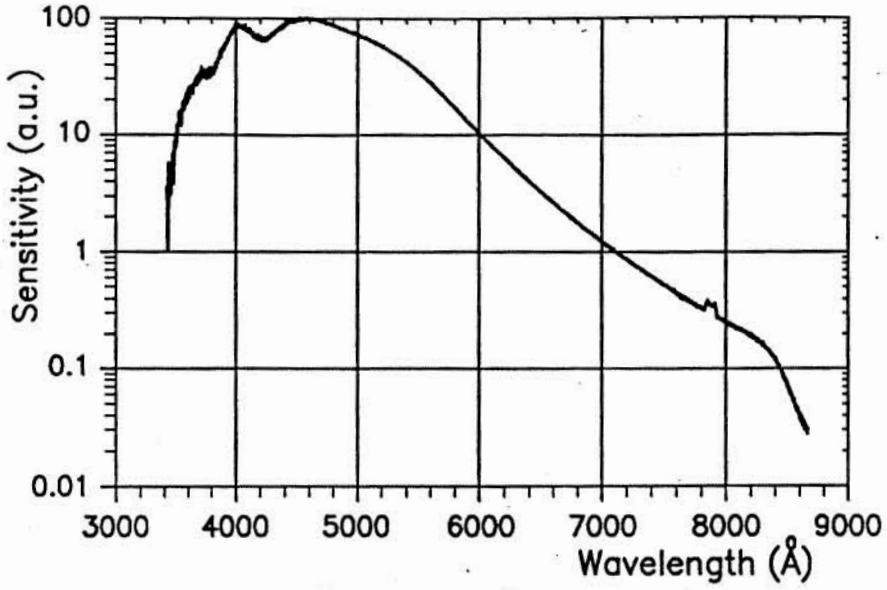


**Figure 3:** Measured sensitivity curve of the combined optical detection system, in arbitrary units.

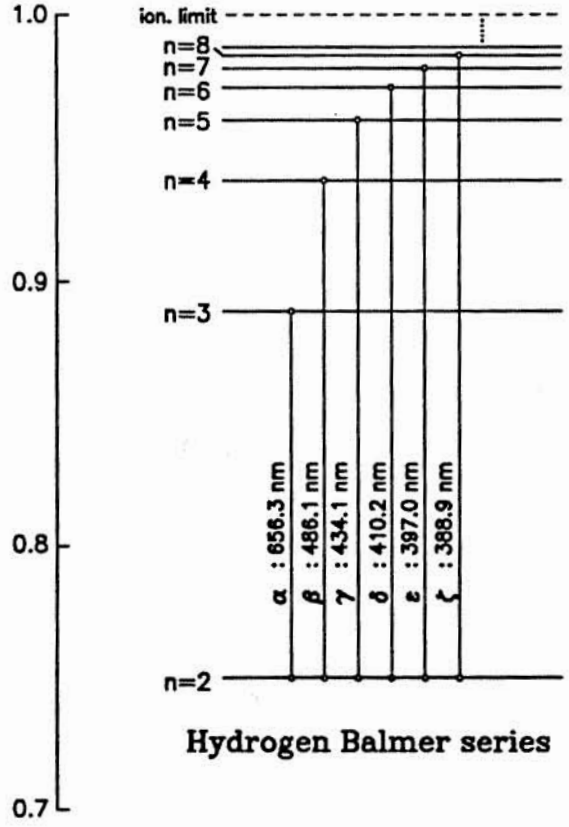


**Figure 4:** Schematic energy level diagram of atomic hydrogen, indicating the transitions of the Balmer series. Numbers along the vertical scale are in units of the ionization potential (13.6 eV).

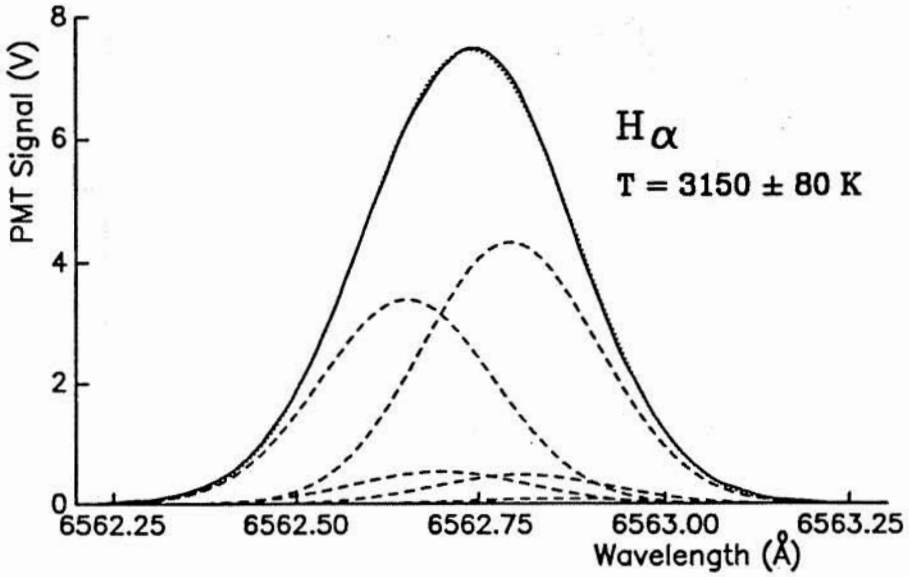


**Figure 5:** Measured emission lineshape of the hydrogen Balmer-alpha line (solid curve). Also shown is a multi-component gaussian curve fit (dotted curve). The individual fine structure components of the fit are shown as dashed curves.

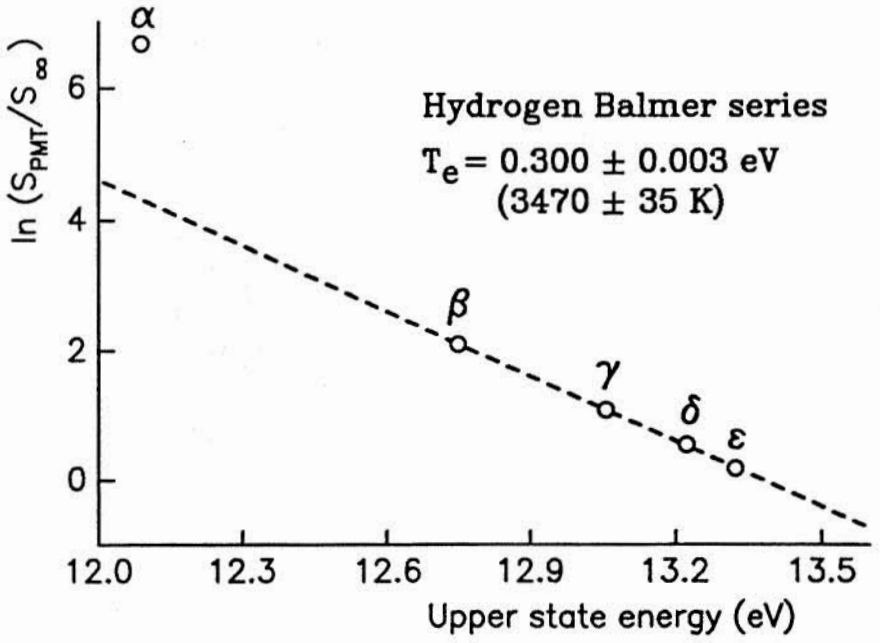


**Figure 6:** Boltzmann plot for the hydrogen Balmer-alpha through Balmer-epsilon lines.

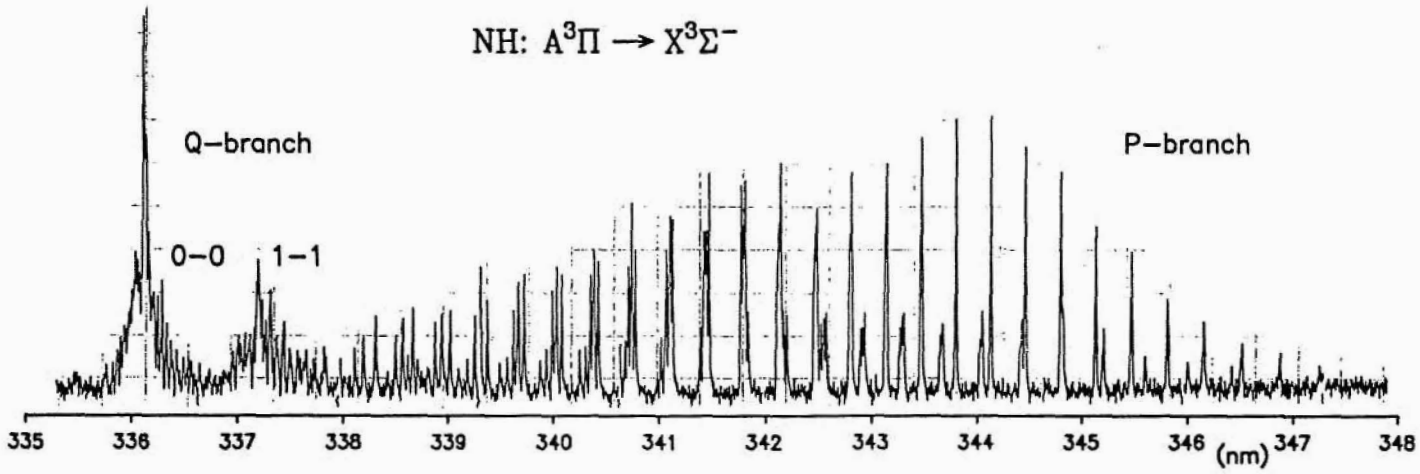


**Figure 7:** Emission scan of the NH $A^3\Pi \rightarrow X^3\Sigma^-$ band, performed about 2 mm downstream from the exit nozzle. Both 0-0 and 1-1 vibrational bands are present.



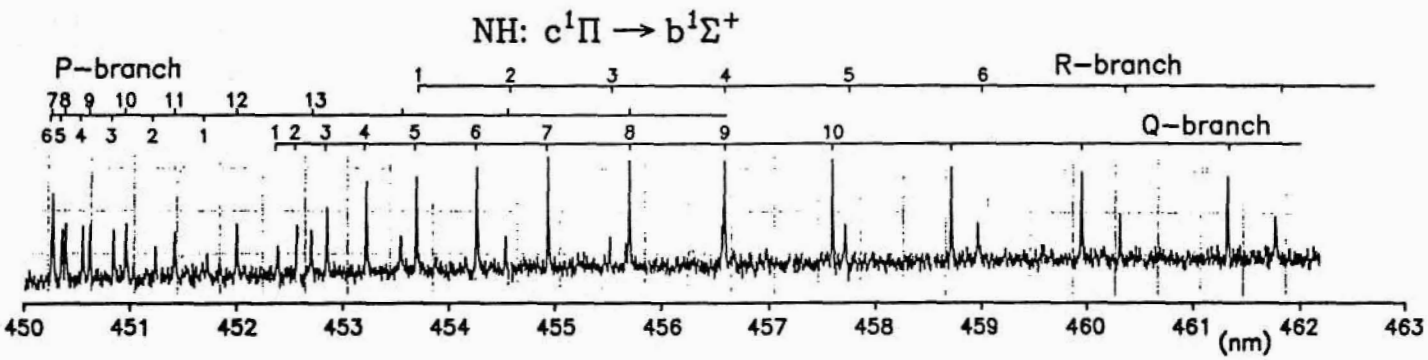


**Figure 8:** Part of the NH $c^1\Pi \rightarrow b^1\Sigma^+$ band, for the same conditions as in Fig. 7. Line designations are indicated.

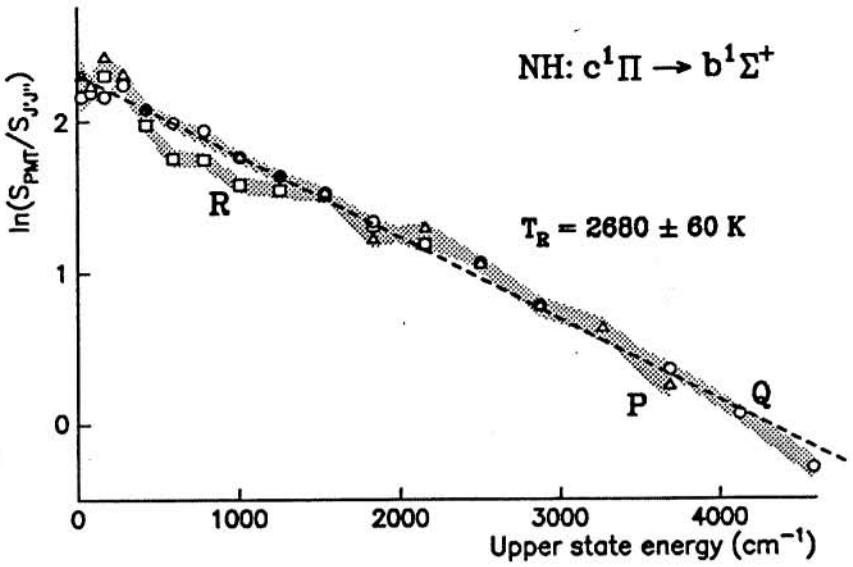


**Figure 9:** Boltzmann plot for the rotational lines of the NH $c^1\Pi \rightarrow b^1\Sigma^+$ band from Fig. 8. Triangular, round, and square data points represent P, Q, and R-branch transitions, respectively. The shaded bands indicate estimated uncertainties of the individual data points.

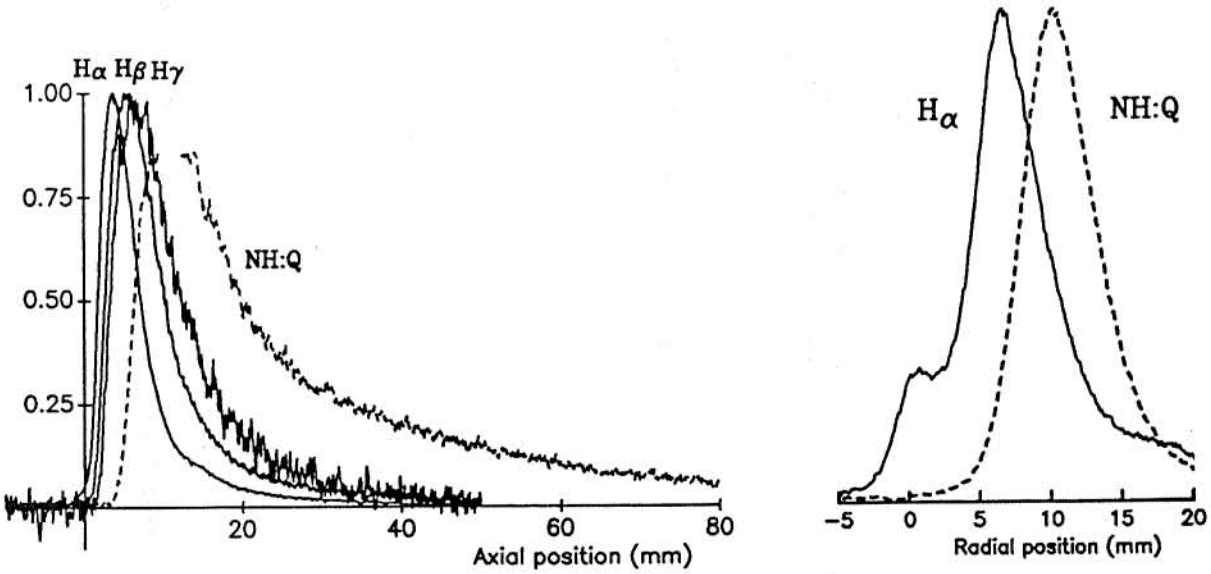


**Figure 10:** Measured axial (left) and radial variation (right) in emission intensity of several plume species. See text for a discussion of the effects of optical distortion.